Front. Phys. 13(2), 130503 (2018)
https://doi.org/10.1007/s11467-017-0737-z

RESEARCH ARTICLE

Chimera states in bipartite networks of FitzHugh–Nagumo oscillators

Zhi-Min Wu[1], Hong-Yan Cheng[1,†], Yuee Feng[2], Hai-Hong Li[1], Qiong-Lin Dai[1], Jun-Zhong Yang[1,‡]

[1] *School of Science, Beijing University of Posts and Telecommunications, Beijing 100876, China*
[2] *Basic Education Department, Jiangsu Aviation Technical College, Zhenjiang 212134, China*
Corresponding authors. E-mail: †hycheng@bupt.edu.cn, ‡jzyang@bupt.edu.cn
Received September 15, 2017; accepted October 29, 2017

Chimera states consisting of spatially coherent and incoherent domains have been observed in different topologies such as rings, spheres, and complex networks. In this paper, we investigate bipartite networks of nonlocally coupled FitzHugh–Nagumo (FHN) oscillators in which the units are allocated evenly to two layers, and FHN units interact with each other only when they are in different layers. We report the existence of chimera states in bipartite networks. Owing to the interplay between chimera states in the two layers, many types of chimera states such as in-phase chimera states, antiphase chimera states, and out-of-phase chimera states are classified. Stability diagrams of several typical chimera states in the coupling strength–coupling radius plane, which show strong multistability of chimera states, are explored.

Keywords chimera states, bipartite networks, FitzHugh–Nagumo oscillators

PACS numbers 05.45.Xt, 05.45.Ra

1 Introduction

A chimera state is an interesting spatiotemporal pattern consisting of spatially separated domains of coherent and incoherent behavior, which was first found by Kuramoto and his colleagues while simulating the nonlocally coupled Ginzburg–Landau equations in 2002 [1–3]. Strogatz later called these patterns chimera states because of their similarity to the mythological Greek beast made up of incongruous parts. Their work showed that the stable chimera state bifurcates from a spatially modulated drift state and dies in a saddle-node bifurcation with an unstable chimera state [4, 5]. The study of chimera states might be helpful for better understanding some complex behaviors in biological [6], engineering [7], and social systems [8] in the real world. For instance, unihemispheric sleep is quite common in the real world; in this state, one cerebral hemisphere shows desynchronized electrical activity, whereas the other is highly synchronized.

Recent research has shown that chimera states can be found not only in phase oscillator systems [9–12] but also in a large variety of systems including neuronal oscillators [13], inertial oscillators [14], and time-discrete chaotic systems [15]. In the one-dimensional FitzHugh–Nagumo (FHN) model with nonlocal coupling, different multicluster chimera states may be identified depending on the coupling strength and coupling range [16]. Recently, coherence-resonance chimeras were proposed by Semenova *et al.*, who applied noise with intermediate strength to excitable FHN systems and found alternating switching of the location of coherent and incoherent domains [17]. Moreover, Isele *et al.* found that introducing excitable units into nonlocally coupled oscillatory units may make it possible to control the position of a chimera state [18].

Chimera states are not restricted to topologies such as rings [4], square lattices [19, 20], tori [21], and spheres [22]. Zhu *et al.* investigated the properties of chimera states on complex networks such as Erdös-Rényi networks and scale-free networks [23]. Yao *et al.* studied the robustness of chimera states against random removal of edges in symmetrically nonlocally coupled rings [24]. A detailed introduction to the effects of different coupling topologies on chimera dynamics can be found in a perspective article [25]. Recently, chimera states in multiplex networks of coupled oscillators have attracted attention. Ghosh *et al.* considered a two-layer network

of chaotic maps in the presence of delayed interactions in which the chaotic maps are nonlocally coupled in each layer, and the interlayer interaction is mediated by one-to-one coupling between the mirror maps on different layers [26]. They found that the interplay of delay and multiplexing results in enhanced or suppressed appearance of the chimera state. Maksimenko and his colleagues found synchronous and asynchronous chimera states by studying a two-layer network of coupled phase oscillators in which phase oscillators in the same layer are coupled nonlocally, and each oscillator in one layer is globally coupled to the other layer [27]. Majhi *et al.* studied a two-layer network of the coupled Hindmarsh–Rose model, in which oscillators are uncoupled in one layer but globally coupled in the other layer, and interaction between layers is represented by one-to-one connections between mirror oscillators [28, 29]. They found an interesting quorum sensing mechanism for chimera states.

The investigation of chimera states in multiplex networks of coupled oscillators [26, 27] suggests a new direction in the field of chimera dynamics by studying the interaction between chimera states present in different subpopulations. Along this line, we investigate chimera dynamics in bipartite networks of nonlocally coupled oscillatory FHN systems in this paper. In network science, a bipartite network is a network whose nodes can be divided into two disjoint subpopulations, where connections exist only between nodes of different subpopulations. Bipartite networks may be treated as a special type of multiplex network in which no interaction exists between nodes in the same layer (or subpopulation). We will show the existence of chimera states in bipartite networks and then the rich chimera dynamics due to the interplay between chimera dynamics in different layers (or subpopulations).

The rest of the paper is organized as follows. We introduce a bipartite network of the nonlocally coupled FHN model in Section 2. In Section 3, we investigate the chimera dynamics in both homogeneous and heterogeneous bipartite networks. Rich chimera dynamics including multistability is revealed. A summary is presented in Section 4.

2 Model

We consider a bipartite network of $2N$ identical FHN units that are evenly divided into two layers (or subpopulations). Units in each layer situate themselves spatially on a ring, and the ith units in layers 1 and 2 are mirror units. There is no interaction between units in the same layer, whereas every unit in layer α ($\alpha = 1, 2$) interacts with $2R_\alpha$ nearest neighbors of its mirror unit in layer β ($\beta \neq \alpha$). The model equation of the bipartite network of nonlocally coupled FHN units is as follows:

$$\begin{aligned}
\varepsilon \dot{u}_i^\alpha &= u_i^\alpha - \frac{(u_i^\alpha)^3}{3} - v_i^\alpha \\
&\quad + \frac{\sigma_\alpha}{2R_\alpha + 1} \sum_{j=i-R_\alpha}^{i+R_\alpha} [C_{uu}(u_j^\beta - u_i^\alpha) + C_{uv}(v_j^\beta - v_i^\alpha)], \\
\dot{v}_i^\alpha &= u_i^\alpha + a \\
&\quad + \frac{\sigma_\alpha}{2R_\alpha + 1} \sum_{j=i-R_\alpha}^{i+R_\alpha} [C_{vu}(u_j^\beta - u_i^\alpha) + C_{vv}(v_j^\beta - v_i^\alpha)].
\end{aligned} \tag{1}$$

The subscript i refers to the unit index, which must be taken modulo N (or a periodic boundary condition). The superscripts α and β indicate layers α and β. u_i^α and v_i^α are the activator and inhibitor variables of unit i on layer α, respectively. The positive parameter ε separates the time scales of the dynamics of the activator and inhibitor variables. σ_α and R_α denote the strength and range, respectively, of nonlocal coupling on layer α exerted by layer β. For convenience, we introduce the coupling radius $r_\alpha = R_\alpha/N$, which ranges from $1/N$ (nearest-neighbor coupling) to 0.5 (global coupling). In reference [16], it was shown that the existence of chimera states in nonlocally coupled FHN oscillators requires cross-coupling between the activator and inhibitor variables in addition to direct $u - u$ and $v - v$ coupling. A simple way to take both types of coupling into account is to model the coupling with a rotational coupling matrix

$$C = \begin{pmatrix} C_{uu} & C_{uv} \\ C_{vu} & C_{vv} \end{pmatrix} = \begin{pmatrix} \cos\phi & \sin\phi \\ -\sin\phi & \cos\phi \end{pmatrix} \tag{2}$$

depending on a single parameter ϕ. An isolated FHN unit generally exhibits excitable behavior for $|a| > 1$ but oscillatory behavior for $|a| < 1$ via a Hopf bifurcation at $|a| = 1$. In this paper, we focus on the oscillatory regime and take $a = 0.5$.

3 Results and analysis

We numerically simulate Eq. (1) using the fourth-order Runge–Kutta method with a time step $\delta t = 0.01$. Throughout the paper, the total oscillator number is set to $2N = 2000$. We also set $\phi = \frac{\pi}{2} - 0.1$ and $\epsilon = 0.05$.

3.1 Homogeneous bipartite networks

In this subsection, we consider homogeneous bipartite networks of FHN units in which $\sigma_1 = \sigma_2 = \sigma$, $r_1 = r_2 = r$ and show rich chimera dynamics in this case. Realization of a chimera state is identified by two methods. Snapshots of the activator variable u show patterns

characterized by smooth curves in coherent domains and scattered points in incoherent domains. The mean phase velocities of FHN units, calculated as $\omega_i = 2\pi M_i/\Delta T$, where M_i is the number of complete rotations around the origin performed by the ith unit during the time interval ΔT, lie on a continuous curve with plateaus corresponding to the coherent domains.

First, we consider initial conditions in which FHN units in both layers are randomly distributed on the circle $u_i^2 + v_i^2 = 4$. The top row in Fig. 1, in which snapshots of the variable u at $t^* = 10\,000$ time units and the mean phase velocities with $\Delta T = 10\,000$ time units are presented, shows that chimera states do exist in homogeneous bipartite networks of FHN units and, in each layer, the FHN units organize themselves into a pattern of a chimera state. We realized 1-cluster, 2-cluster, and 3-cluster chimera states for three combinations of σ and r. Interestingly, the patterns of chimera states in each layer seem the same as those in a ring of nonlocally coupled FHN units with the same parameters, as shown by both the snapshots of the variable u and the profiles of the mean phase velocity. Furthermore, the chimera states in the two layers are spatially in phase. By "spatially in phase", we mean that the coherent/incoherent domains in the two layers have the same locations, and coherent units from different layers are in phase if they are mirror ones. In contrast to the synchronous chimera states in two-layer multiplex networks [27], the mirror units in incoherent domains can be both synchronized and desynchronized here. The chimera states in homogeneous bipartite networks in the top row of Fig. 1 are the counterparts of the multicluster chimera states in rings of nonlocally coupled FHN units, and we call them normal in-phase multicluster chimera states. As shown

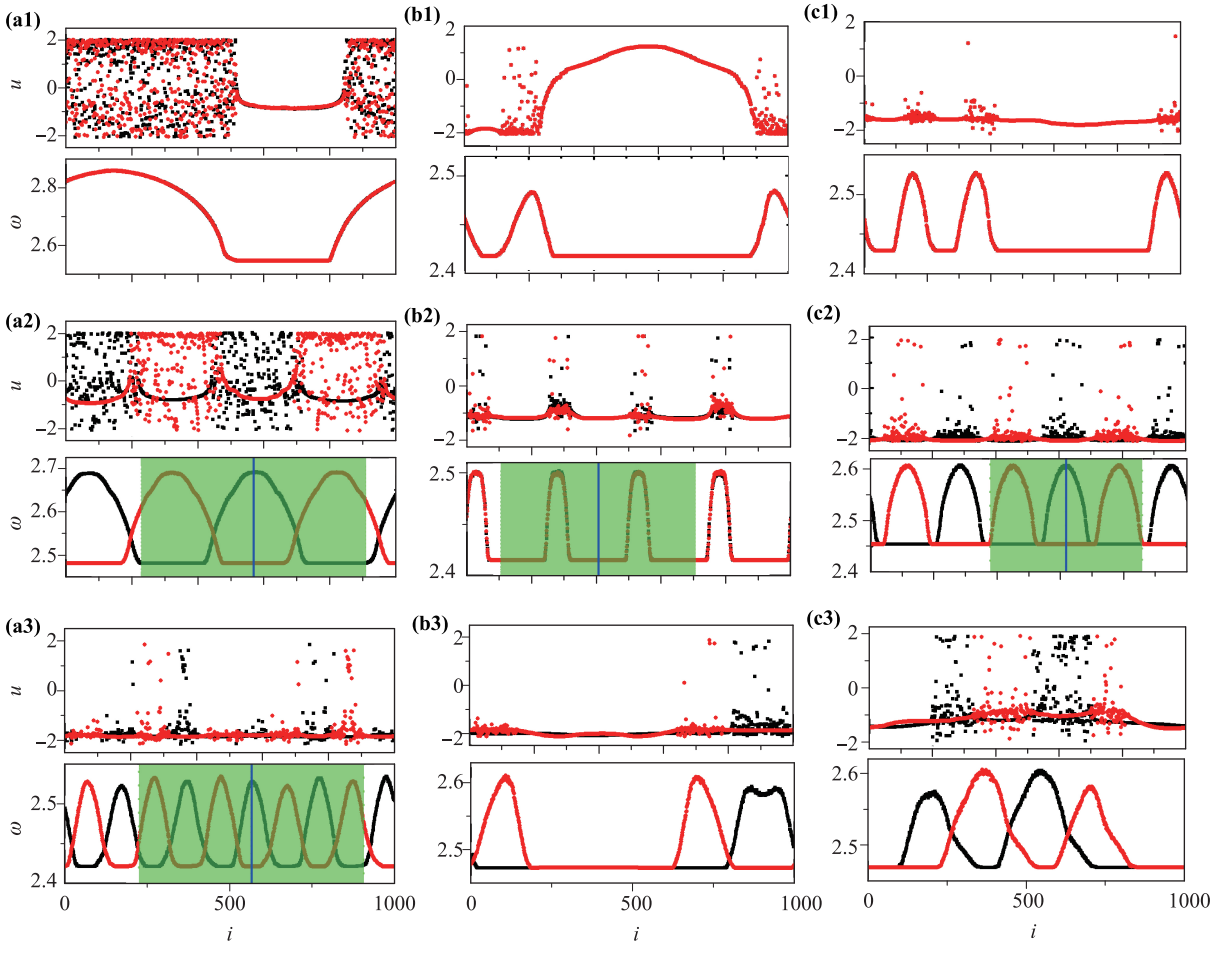

Fig. 1 Different types of chimera states in homogeneous bipartite networks of nonlocally coupled FHN units. In each panel, the top plot shows a snapshot of the variable u, and the bottom one shows the corresponding mean phase velocity ω. In each plot, the FHN units in layer 1 are black, and those in layer 2 are red. The coupling strength and coupling radius in each column are the same. **(a1–a3)** $r = 0.34$ and $\sigma = 0.18$; **(b1–b3)** $r = 0.30$ and $\sigma = 0.30$; **(c1–c3)** $r = 0.24$ and $\sigma = 0.26$. In (a2), (a3), (b2), and (c2), the blue solid line denotes a focal FHN unit, and the green region represents its coupling range in the other layer.

in the top row of Fig. 1, decreasing the coupling radius increases the number of coherent domains in normal in-phase multicluster chimera states.

In a ring of nonlocally coupled FHN units, multistability always appears near the borders of parameter regimes supporting typical chimera dynamics. Multistability also exists in homogeneous bipartite networks. To show this, we prepare initial conditions by using the normal in-phase multichimera states $\{(u_i^\alpha(t^*), v_i^\alpha(t^*))\}$ in the top row in Fig. 1. We set the initial conditions to $u_i^1(t=0) = u_i^1(t^*)$ and $v_i^1(t=0) = u_i^1(t^*)$ in layer 1 and $u_i^2(t=0) = u_{i+k}^2(t^*)$ and $v_i^2(t=0) = u_{i+k}^2(t^*)$ in layer 2, where the values of k are multiples of 100. Namely, we dislocate the chimera states in the two layers by a distance k. By adopting different k, different type of chimera dynamics may be developed, and some typical chimera states are presented in the middle and bottom rows in Fig. 1.

Starting with the normal in-phase chimera state with one coherent/incoherent domain in Fig. 1(a1), the dislocation of chimera states in the two layers may give rise to the multichimera states with two coherent domains in Fig. 1(a2) and with five coherent domains in Fig. 1(a3) for the same combination of σ and r. Interestingly, these multichimera states are spatially antiphase, where the mirror FHN units of coherent/incoherent domains in one layer are always incoherent/coherent in the other layer. We may call these chimera states antiphase multicluster chimera states. Note that, in an antiphase chimera state, all the coherent/incoherent domains have nearly the same size, and coherent units have the same mean phase velocity. Dislocation of the normal in-phase multicluster chimera state in Fig. 1(b1) may lead to other types of chimera states. Figure 1(b2) shows a multicluster chimera state with four coherent and four incoherent domains. All of these coherent/incoherent domains have the same size. In contrast to the antiphase multicluster chimera states in Figs. 1(a2) and (a3), the mirror units of the coherent/incoherent domains in one layer must behave coherently/incoherently in the other layer. That is, we find a new type of spatially in-phase multichimera state that has no counterpart in a ring of nonlocally coupled FHN units, and we call it an abnormal in-phase multicluster chimera state. Moreover, Fig. 1(b3) shows an interesting chimera dynamics in which the numbers of coherent domains in the two layers are different. We call the state a 1-2-cluster chimera state. Further, Figs. 1(c2) and (c3) show that the normal in-phase 3-cluster chimera state in Fig. 1(c1) coexists with an antiphase 3-cluster chimera state in Fig. 1(c2) and another type of multicluster chimera state with two coherent/incoherent domains in each layer in Fig. 1(c3). The 2-cluster chimera state in Fig. 1(c3) may be called an out-of-phase 2-cluster chimera state because, geometrically, the state resembles a dislocated normal in-phase 2-cluster chimera state.

So far, we have identified several types of chimera states in bipartite networks of nonlocally coupled FHN units. Before proceeding, some points should be discussed. First, it has to be stressed that buildup of chimera states in bipartite networks is mediated by the interaction between the two layers. Second, the number n of coherent domains increases with decreasing coupling radius for n-cluster chimera states in a ring of FHN units. However, no such simple relation exists between the number of coherent domains and the coupling radius, which is demonstrated in Figs. 1(a2) and (c3). Third, we have found antiphase n-cluster chimera states and abnormal in-phase n-cluster chimera states. Thus, a question arises. Can an antiphase n-cluster chimera state coexist with an abnormal in-phase n-cluster chimera state? Extensive numerical simulations have shown that the answer is no. A heuristic explanation is as follows, taking the antiphase 2-cluster chimera state in Fig. 1(a2) as an example. Generally, a unit in a chimera state is most likely to be coherent/incoherent if it receives more input from coherent/incoherent units than from incoherent/coherent ones. Consider a coherent/incoherent FHN unit in Fig. 1(a2), which is denoted by a blue solid line; its coupling range is shown in green. When the underlying state is an antiphase 2-cluster chimera state, its mirror unit has more coherent/incoherent neighbors than incoherent/coherent ones, which is compatible with its coherent/incoherent dynamics. Now, suppose that the underlying state could be an abnormal in-phase 2-cluster chimera state. We will find that the mirror unit of the focal coherent one has more incoherent neighbors, which will turn the focal unit incoherent. Following this logic, we know that coexistence of an antiphase n-cluster chimera state and an abnormal in-phase n-cluster chimera state is impossible. Finally, rich chimera states in bipartite networks, which are probably induced by the interaction between chimera states in the two layers in bipartite networks, have not been observed in a ring of FHN units.

To gain an overview of chimera dynamics in bipartite networks of FHN units, we explore the r–σ plane. We use the chimera states in Fig. 1 as initial conditions and integrate Eq. (1) for 10^4 time units. We classify the chimera states realized after this interval as stable. (Note that there are other methods of investigating the stability of chimera states, such as the method of basin stability [30]). Figure 2 shows the stability diagrams of several types of chimera states in bipartite networks of nonlocally coupled FHN units, where the multistability dominates in the r–σ plane. Bearing in mind that the normal in-phase multicluster chimera states are the counterparts of n-cluster chimera states in a ring of FHN units, we find that the stability diagrams of these chimera states

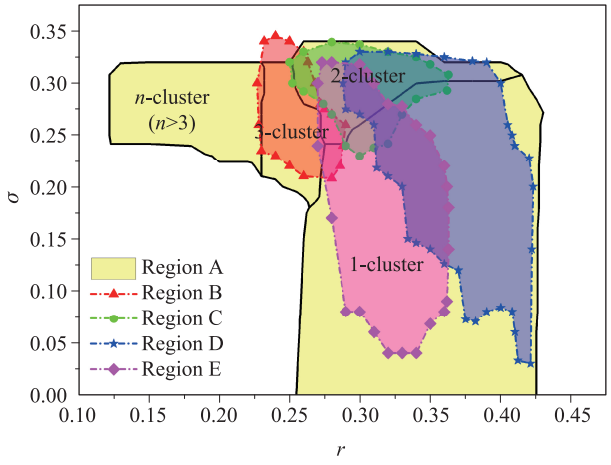

Fig. 2 Stability diagrams for different types of chimera states in the r–σ plane in homogeneous bipartite networks of nonlocally coupled FHN units. The region A in yellow allows for normal in-phase n-cluster chimera states and is subdivided into four regions for normal in-phase 1-cluster, 2-cluster, 3-cluster, and $n > 3$-cluster chimera states. The regions for the out-of-phase 2-cluster chimera state, 1-2-cluster chimera state, antiphase 2-cluster chimera state, and abnormal in-phase 4-cluster chimera state are labeled B, C, D, and E, respectively.

are similar in these two systems despite the slight discrepancy in their boundaries. For example, the normal in-phase 1-cluster chimera state appears at large r and is dominant for weak coupling strength. On the other hand, normal in-phase multicluster chimera states require sufficiently strong coupling strength, and reducing r increases the number of coherent clusters. Note that, for convenience of illustration, we ignore the coexistence of normal in-phase multicluster chimera states. Figure 2 also presents the stability diagrams for the abnormal in-phase 4-cluster chimera state, antiphase 2-cluster chimera state, out-of-phase chimera state, and 1-2-cluster chimera state. In contrast to the out-of-phase chimera state and 1-2-cluster chimera state, which require strong coupling, the abnormal in-phase 4-cluster chimera state and antiphase 2-cluster chimera state can be realized at sufficiently weak coupling strength. Interestingly, the abnormal in-phase 4-cluster chimera state can be realized at a larger coupling radius than the antiphase 2-cluster chimera state, which further convinces us that there is no simple relation between the coupling radius and the number of coherent domains in bipartite networks. Figure 2 reveals strong multistability in bipartite networks of FHN units. Multistability exists in most of the parameter regions supporting chimera states, and, in certain regions, more than four types of chimera states coexist.

3.2 Heterogeneous bipartite networks

In this subsection, we consider heterogeneous bipartite networks of FHN units in which $\sigma_1 = \sigma_2$ and $r_1 = r_2$ are not required. Surprisingly, the asymmetry between the two layers suppresses the formation of certain types of chimera states. For example, if the coupling strength and coupling radius in the two layers are kept within their stable regions for homogeneous bipartite networks, the abnormal in-phase 4-cluster chimera state cannot be realized even in the presence of weak heterogeneity for the two layers. Nevertheless, like homogeneous bipartite networks, heterogeneous bipartite networks still display strong multistability.

To show multistability in heterogeneous bipartite networks, we consider two parameter paths, on which the coupling radius is varied for a fixed coupling strength and the coupling strength is varied for a fixed coupling radius. Along these paths, we consider 60 sets of initial conditions for each combination of r and σ prepared by dislocating by k (in multiples of 100) the chimera states in the middle and bottom rows in Fig. 1. The possible states resulting from these initial conditions are presented in the rightmost two columns in Fig. 3. For clarity, we numbered these states. For example, the state assigned to the integer 1 is a traveling wave with wave number 1, and the state labeled 2 is a traveling wave with wave number 3. In addition to the typical chimera states already presented in Fig. 1, we find another type of chimera state, the state labeled 3, in which the model displays chimera dynamics in one layer and coherent dynamics in the other layer. Figure 3(a) shows the chimera states labeled with each integer against r_1 with $\sigma_1 = \sigma_2 = 0.275$ and $r_2 = 0.24$. We find that chimera states tend to disappear when the difference between r_1 and r_2 becomes large. When $|r_1 - r_2|$ is not too large, there are always several types of chimera states coexisting with each other. Furthermore, multistability is also observed in Fig. 3(b), where the chimera states are plotted against σ_1 for $r_1 = r_2 = 0.24$ and $\sigma_2 = 0.275$. The results in Fig. 3 suggest that the multistability tends to be stronger when bipartite networks are less heterogeneous.

Then, we study the effects of the heterogeneity of bipartite networks on the properties of chimera states, such as the sizes of the coherent domains and the maximum/minimum mean phase velocities. The stability diagrams in Fig. 2 for homogeneous bipartite networks show that variation of the coupling radius tends to change the type of chimera states. Therefore, we focus on the effects of heterogeneity in the coupling strength on the properties of chimera states. We set the coupling radius $r_1 = r_2 = 0.35$ and $\sigma_2 = 0.20$. Starting with the normal in-phase 1-cluster chimera state and the antiphase

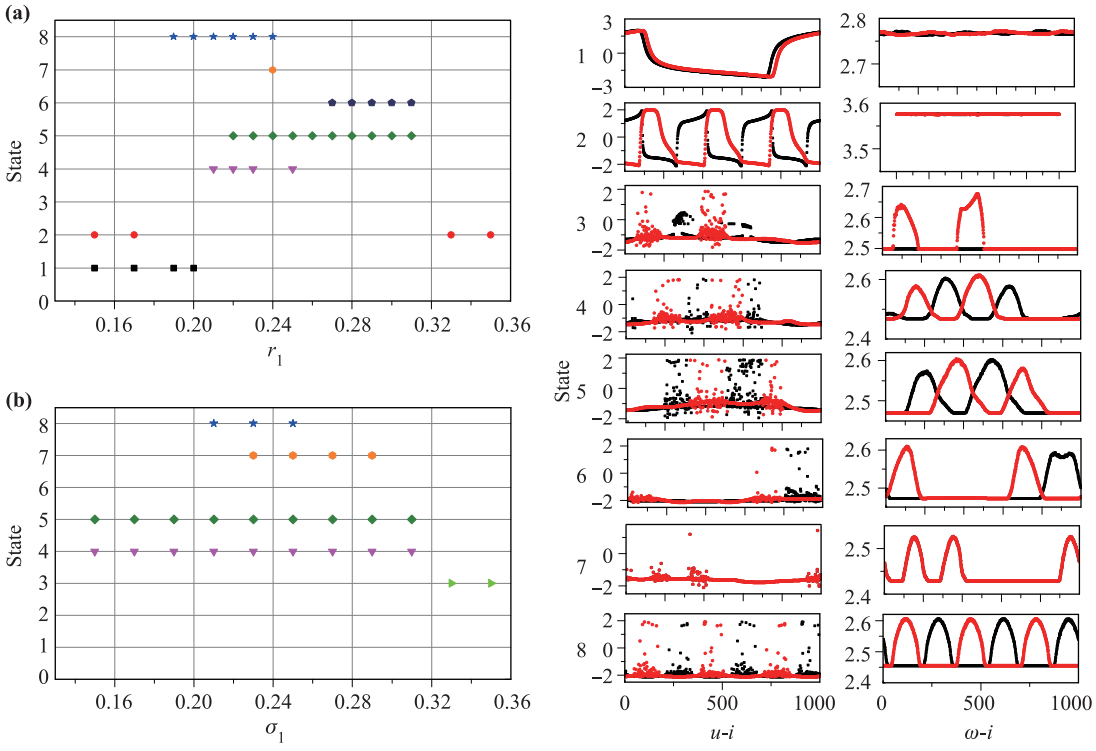

Fig. 3 Possible dynamical states labeled with different integers are plotted against r_1 with $\sigma_1 = \sigma_2 = 0.275$ and $r_2 = 0.24$ in **(a)** and against σ_1 with $r_1 = r_2 = 0.24$ and $\sigma_2 = 0.275$ in **(b)**. The middle and right columns show snapshots of the variable u and profiles of the mean phase velocity for all possible dynamical states, respectively, and the integers assigned to those states appear on the left side of the middle column. The possible dynamical states include the traveling wave state with wave number 1 (the state labeled 1), the traveling wave state with wave number 3 (state 2), the state having a chimera state in one layer and a coherent state in the other layer (state 3), the out-of-phase 3-cluster chimera state (state 4), the out-of-phase 2-cluster chimera state (state 5), the 1-2-cluster chimera state (state 6), the normal in-phase chimera state (state 7), and the antiphase 3-cluster chimera state (state 8).

2-cluster chimera state in Fig. 1 as initial conditions, the properties of the corresponding chimera states are presented with increasing σ_1 in Figs. 4(a1), (a2) and (b1), (b2), respectively. Generally, the layer with large coupling strength has larger coherent domains, which can be deduced by noticing that σ_α represents the coupling strength on layer α exerted by layer β ($\beta \neq \alpha$), and the dependence of the sizes of the coherent domains on σ_1 is sensitive to the underlying dynamical states. Figure 4(a1) shows that, when $\sigma_1 < 0.23$, the size of the coherent domain in layer 1 (or layer 2) increases (or decreases) with increasing σ, whereas the total size of the coherent domains in the two layers remains unchanged. However, for $\sigma_1 > 0.23$, the sizes of the coherent domains show nonmonotonic behavior with respect to σ_1. Examining the chimera states during the process, we find that normal in-phase 1-cluster chimera states exist for $\sigma < 0.23$, whereas, for $\sigma_1 > 0.23$, the normal in-phase 1-cluster chimera state is becoming a normal in-phase 2-cluster one [16]. The insets in Fig. 4(a1) show the corresponding chimera states at $\sigma_1 = 0.12$ and $\sigma_1 = 0.28$. On the other hand, Fig. 4(b1) shows that, for antiphase 2-cluster chimera states, the total size of the coherent domains in the two layers increases with σ_1, and the sizes of the coherent domains in both layers are nondecreasing functions of σ_1. Figures 4(a2) and (b2) show the maximum/minimum mean phase velocities. Here, the minimum mean phase velocities are exhibited by coherent FHN units, and the maximum mean phase velocities are exhibited by incoherent units. Clearly, the dependence of the maximum/minimum mean phase velocities on the coupling strength is also determined by the underlying chimera states.

4 Conclusions

In conclusion, we showed the existence of chimera states in bipartite networks of nonlocally coupled FHN units in which the FHN units interact with each other only when they are in different layers. We observed rich chimera dynamics and strong multistability in bipartite

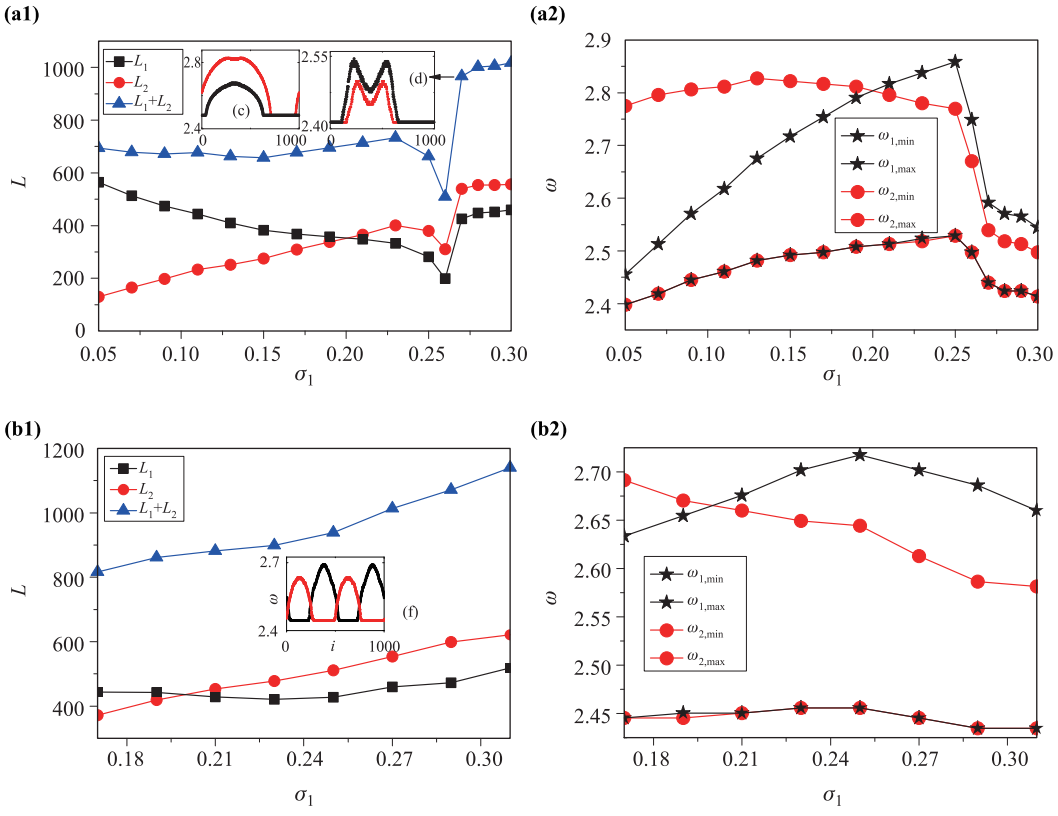

Fig. 4 Sizes $L_{1,2}$ of coherent domains in layers 1 and 2 and the total size $L_1 + L_2$ are plotted against σ_1 in **(a1)** for normal in-phase 1-cluster chimera states and in **(b1)** for antiphase 2-cluster chimera states. The corresponding minima and maxima of the mean phase velocities ω in the two layers are plotted against σ_1 in **(a2)** and **(b2)**, respectively. $r_1 = r_2 = 0.35$, $\sigma_2 = 0.20$. Insets (c)(d) in (a1) show the mean phase velocities at $\sigma_1 = 0.12$ and $\sigma_1 = 0.28$, respectively. Inset (f) in (b1) shows the mean phase velocities at $\sigma_1 = 0.23$.

networks. For homogeneous bipartite networks, where the FHN units in the two layers have the same parameters, we found the chimera dynamics observed in previous works, such as the counterparts of chimera states in a ring of nonlocally coupled FHN units (normal in-phase multicluster chimera states) and antiphase multicluster chimera states. We also found many novel types of chimera states due to the interplay between chimera states in the two layers, for example, abnormal in-phase multicluster chimera states and out-of-phase chimera states. The stability diagrams of several typical chimera states, which demonstrated strong multistability of chimera dynamics in bipartite networks, were explored. For heterogeneous bipartite networks, where the FHN units in the two layers may have different parameters, we found strong multistability of chimera states even when the presence of heterogeneity disfavors some types of chimera states. Many previous works have shown that the number of coherent clusters is determined by the coupling range; for example, reducing the coupling range leads to an increase in the number of coherent clusters. However, this work shows a different picture; an increase in the number of coherent clusters may be assisted by the interaction between chimera dynamics in different subpopulations even when the coupling range is unchanged.

Acknowledgements This work was supported by the National Natural Science Foundation of China under Grant Nos. 11575036 and 11505016.

References

1. Y. Kuramoto and D. Battogtokh, Coexistence of coherence and incoherence in nonlocally coupled phase oscillators, *Nonlinear Phenom. Complex Syst.* 5, 380 (2002), arXiv: cond-mat/0210694
2. D. Tanaka and Y. Kuramoto, Complex Ginzburg-Landau equation with nonlocal coupling, *Phys. Rev. E* 68(2), 026219 (2003)
3. S. I. Shima and Y. Kuramoto, Rotating spiral waves with phase-randomized core in nonlocally coupled oscillators, *Phys. Rev. E* 69(3), 036213 (2004)

4. D. M. Abrams and S. H. Strogatz, Chimera states for coupled oscillators, *Phys. Rev. Lett.* 93(17), 174102 (2004)
5. D. M. Abrams and S. H. Strogatz, Chimera states in a ring of nonlocally coupled oscillators, *Int. J. Bifurcat. Chaos* 16(01), 21 (2006)
6. N. C. Rattenborg, C. J. Amlaner, and S. L. Lima, Behavioral, neurophysiological and evolutionary perspectives on unihemispheric sleep, *Neurosci. Biobehav. Rev.* 24(8), 817 (2000)
7. A. E. Motter, S. A. Myers, M. Anghel, and T. Nishikawa, Spontaneous synchrony in power-grid networks, *Nat. Phys.* 9(3), 191 (2013)
8. J. C. González-Avella, M. G. Cosenza, and M. San Miguel, Localized coherence in two interacting populations of social agents, *Physica A* 399, 24 (2014)
9. D. M. Abrams, R. Mirollo, S. H. Strogatz, and D. A. Wiley, Solvable model for chimera states of coupled oscillators, *Phys. Rev. Lett.* 101(8), 084103 (2008)
10. G. C. Sethia, A. Sen, and F. M. Atay, Clustered chimera states in delay-coupled oscillator systems, *Phys. Rev. Lett.* 100(14), 144102 (2008)
11. Y. Zhu, Y. Li, M. Zhang, and J. Yang, The oscillating two-cluster chimera state in non-locally coupled phase oscillators, *Europhys. Lett.* 97(1), 10009 (2012)
12. C. R. Laing, The dynamics of chimera states in heterogeneous Kuramoto networks, *Physica D* 238(16), 1569(2009)
13. C. H. Tian, X. Y. Zhang, Z. H. Wang, and Z. H. Liu, Diversity of chimera-like patterns from a model of 2D arrays of neurons with nonlocal coupling, *Front. Phys.* 12(3), 128904 (2017)
14. T. Bountis, V. G. Kanas, J. Hizanidis, and A. Bezerianos, Chimera states in a two–population network of coupled pendulum–like elements, *Eur. Phys. J. Spec. Top.* 223(4), 721 (2014)
15. I. Omelchenko, Y. Maistrenko, P. Hövel, and E. Schöll, Loss of coherence in dynamical networks: Spatial chaos and chimera states, *Phys. Rev. Lett.* 106(23), 234102 (2011)
16. I. Omelchenko, O. E. Omelchenko, P. Hövel, and E. Schöll, When nonlocal coupling between oscillators becomes stronger: Patched synchrony or multichimera states, *Phys. Rev. Lett.* 110(22), 224101 (2013)
17. N. Semenova, A. Zakharova, V. Anishchenko, and E. Schöll, Coherence-resonance chimeras in a network of excitable elements, *Phys. Rev. Lett.* 117(1), 014102 (2016)
18. T. Isele, J. Hizanidis, A. Provata, and P. Hövel, Controlling chimera states: The influence of excitable units, *Phys. Rev. E* 93(2), 022217 (2016)
19. E. A. Martens, C. R. Laing, and S. H. Strogatz, Solvable model of spiral wave chimeras, *Phys. Rev. Lett.* 104(4), 044101 (2010)
20. C. Gu, G. St-Yves, and J. Davidsen, Spiral wave chimeras in complex oscillatory and chaotic systems, *Phys. Rev. Lett.* 111(13), 134101 (2013)
21. M. J. Panaggio and D. M. Abrams, Chimera states on a flat torus, *Phys. Rev. Lett.* 110(9), 094102 (2013)
22. M. J. Panaggio and D. M. Abrams, Chimera states on the surface of a sphere, *Phys. Rev. E* 91(2), 022909 (2015)
23. Y. Zhu, Z. Zheng, and J. Yang, Chimera states on complex networks, *Phys. Rev. E* 89(2), 022914 (2014)
24. N. Yao, Z. G. Huang, Y. C. Lai, and Z. G. Zheng, Robustness of chimera states in complex dynamical systems, *Sci. Rep.* 3(1), 3522 (2013)
25. B. K. Bera, S. Majhi, D. Ghosh, and M. Perc, Chimera states: Effects of different coupling topologies, *EPL* 118(1), 10001 (2017)
26. S. Ghosh, A. Kumar, A. Zakharova, and S. Jalan, Birth and death of chimera: Interplay of delay and multiplexing, *EPL* 115(6), 60005 (2016)
27. V. A. Maksimenko, V. V. Makarov, B. K. Bera, D. Ghosh, S. K. Dana, M. V. Goremyko, N. S. Frolov, A. A. Koronovskii, and A. E. Hramov, Excitation and suppression of chimera states by multiplexing, *Phys. Rev. E* 94(5), 052205 (2016)
28. S. Majhi, M. Perc, and D. Ghosh, Chimera states in uncoupled neurons induced by a multilayer structure, *Sci. Rep.* 6(1), 39033 (2016)
29. S. Majhi, M. Perc, and D. Ghosh, Chimera states in a multilayer network of coupled and uncoupled neurons, *Chaos* 27(7), 073109 (2017)
30. S. Rakshit, B. K. Bera, M. Perc, and D. Ghosh, Basin stability for chimera states, *Sci. Rep.* 7(1), 2412 (2017)